2009

AC susceptibility studies of magnetic relaxation in nanoparticles of Ni dispersed in silica

V. Singh

M. S. Seehra

J. Bonevich

ac susceptibility studies of magnetic relaxation in nanoparticles of Ni dispersed in silica

V. Singh, M. S. Seehra, and J. Bonevich

Citation: Journal of Applied Physics **105**, 07B518 (2009); doi: 10.1063/1.3073949
View online: https://doi.org/10.1063/1.3073949
View Table of Contents: http://aip.scitation.org/toc/jap/105/7
Published by the American Institute of Physics

ac susceptibility studies of magnetic relaxation in nanoparticles of Ni dispersed in silica

V. Singh,[1] M. S. Seehra,[1,a)] and J. Bonevich[2]
[1]*Department of Physics, West Virginia University, Morgantown, West Virginia 26506, USA*
[2]*National Institute of Standards and Technology, Gaithersburg, Maryland 20899, USA*

(Presented 13 November 2008; received 5 September 2008; accepted 7 December 2008; published online 25 February 2009)

Temperature dependence of ac susceptibilities χ' and χ'' are reported using frequencies f_m=0.1, 1, 99, 499, and 997 Hz for nanoparticles of Ni dispersed in silica (Ni/SiO_2: 15/85) with the mean sizes D=3.8, 11.7, 15, and 21 nm ($\sigma \simeq 0.2$ nm), as determined by transmission electron microscopy. The blocking temperatures T_B, as determined by peaks in χ'' versus T data, are fit to the Vogel–Fulcher law based on the following equation: $T_B = T_o + T_a/\ln(f_o/f_m)$. Using the attempt frequency $f_o = 1.82 \times 10^{10}$ Hz, T_a (K)=310 (21), 954(17), 1334(14), and 1405(47) are determined for D=3.8, 11.7, 15, and 21 nm, respectively, along with T_o (representing the interparticle interaction)=0, 0, 6.6(0.7), and 12.5(2.5) K respectively. The magnitudes of $T_a = K_a V/k$ yield the anisotropy constant K_a increasing with decreasing D (or volume V) due to contributions from surface anisotropy. The validity of the theoretical result $\chi'' = C\,\partial(\chi' T)/\partial T$ with $C \simeq \pi/[2\ln(f_o/2\pi f_m)]$ is checked and the calculated values of f_o are consistent with experimental value of $f_o = 1.82 \times 10^{10}$ Hz. © *2009 American Institute of Physics*. [DOI: 10.1063/1.3073949]

I. INTRODUCTION

Among several factors that affect the measured properties of magnetic nanoparticles (NPs) include size and size distribution, magnetic field H, temperature T, interparticle interactions (IPIs), and the time scale or frequency f_m of measurements.[1,2] The intrinsic anisotropy K_a, which is often size dependent due to different contributions from bulk anisotropy K_b and surface anisotropy K_s, also has major effect on the observed magnetic properties.[3–6] In this work, we report our investigations of the magnetic relaxation of Ni NPs (chemically dispersed in silica) with average particle diameters D=3.8, 11.7, 15, and 21 nm by measuring the temperature dependence of the ac susceptibilities χ' and χ'' at f_m =0.1, 1, 99, 499, and 997 Hz. The particles were synthesized via the citric acid sol-gel route with the Ni/SiO_2 composition of 15/85 (Ref. 7) in order to increase the interparticle separation and hence reduce the IPI.

For noninteracting NPs subjected to a slowly oscillating magnetic field $h = h_o \cos \omega_m t$, χ' and χ'' are given by[2,8]

$$\chi' = \chi_o/[1 + (\omega_m \tau)^2], \tag{1}$$

$$\chi'' = \chi_o \omega_m \tau/[1 + (\omega_m \tau)^2], \tag{2}$$

where the relaxation frequency $f = 1/\tau$ is given by[1,2]

$$f = f_o \exp(-T_a/T). \tag{3}$$

Here $T_a = K_a V/k$ for a particle of volume V with k being the Boltzmann constant, χ_o is the static susceptibility for $\omega \to 0$, $\omega_m = 2\pi f_m$ and f_o is the attempt frequency. For random orientation of the easy axis of the particles each with magnetic moment $\mu = M_s V$, χ' and χ'' of Eqs. (1) and (2) can be written as[8]

$$\chi' = (M_s^2/3K_a)[1 + (T_a/T)\{1/[1 + (\omega_m \tau)^2]\}], \tag{4}$$

$$\chi'' = (M_s^2/3K_a)[(T_a/T)\{\omega_m \tau/[1 + (\omega_m \tau)^2]\}]. \tag{5}$$

The blocking temperature T_B of the particles is determined from Eq. (3) for $f = f_m$ yielding

$$T_B = T_a/\ln(f_o/f_m). \tag{6}$$

In the presence of weak IPI, Eq. (6) is replaced by Eq. (7) below, derived from the Vogel–Fulcher law,[9–11]

$$T_B = T_o + T_a/\ln(f_o/f_m). \tag{7}$$

Here T_o measures the strength of IPI. According to Eq. (6), T_B should increase with increase in f_m. Also from the above equations, it can be shown that χ'' peaks at $\omega_m \tau = 1$ and χ' and χ'' are related by[2]

$$\chi'' = C\,\partial(\chi' T)/\partial T, \tag{8}$$

where $C \simeq \pi/[2\ln(f_o/2\pi f_m)]$. In this work, the above equations are used to interpret the frequency dependence of χ' and χ'' and determine T_B, f_o, and T_a and their variations with the change in the size of the Ni NPs. We also check the validity of Eq. (8)

II. EXPERIMENTAL RESULTS AND DISCUSSION

The NPs of Ni/SiO_2 (15/85) were synthesized following the procedure outlines in an earlier paper.[7] Annealing the samples at 400, 500, 600, and 700 °C for 2 h in ultrahigh purity N_2 gas produced particles of average size D =3.8(0.2), 11.7(0.2), 15(0.2) and 21(0.12) nm as determined by transmission electron microscopy (TEM). In Fig. 1, we show the representative TEM for the 21 nm NPs with log-

a)Author to whom correspondence should be addressed. Electronic mail: mseehra@wvu.edu.

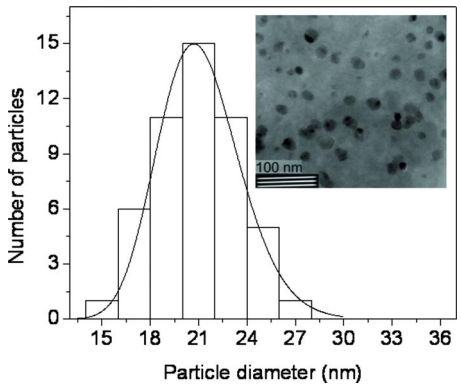

FIG. 1. (Color online) Inset shows the TEM micrograph for the $D=21$ nm sample. The solid line is a fit to log-normal distribution of the histogram of particle sizes.

normal fit to the histogram of the particle sizes. The x-ray diffraction (XRD) patterns for all four sizes using Cu $K\alpha$ source ($\lambda=0.154185$ nm) showed lines only due to fcc Ni and a broad line near $2\theta \simeq 22°$ due to amorphous silica. The sizes determined from the Scherrer broadening of the XRD lines were consistent with the above sizes determined from TEM. Measurements of χ' and χ'' were done using a commercial superconducting quantum interference device magnetometer with the measuring $h_o=7$ Oe and at frequencies $f_m=0.1$, 1, 99, 499, and 997 Hz. These measured value of χ' and χ'' were normalized to 15% concentration of Ni in the Ni/SiO_2 (15/85) samples

For one representative samples with size $D=21$ nm, plots of experimental χ' and χ'' versus T are shown in Fig. 2. Similar data were obtained for the other three samples. It is evident that T_B determined by the peak in χ'' increases with increase in f_m, as predicted by Eqs. (6) and (7). Peaks in χ' are broad and occur at temperatures higher than those for χ'' in agreement with the prediction $\chi''=-(\pi/2)\partial(\ln \chi')/\partial \ln \omega$.[2]

Using the measured values of T_B for each f_m, we plot in Fig. 3 $\ell n f_m$ versus T_B^{-1} following Eq. (6) rewritten as $\ell n f_m = \ell n f_o - (T_a/T_B)$. The data fit the predicted linear behavior with the intercept yielding $\ell n f_o$ and the slope yielding T_a. Using least-squares fitting of the data shown in Fig. 3, the magnitudes of f_o are determined to be $2.83(^{+11.6}_{-2.2})\times 10^9$ Hz

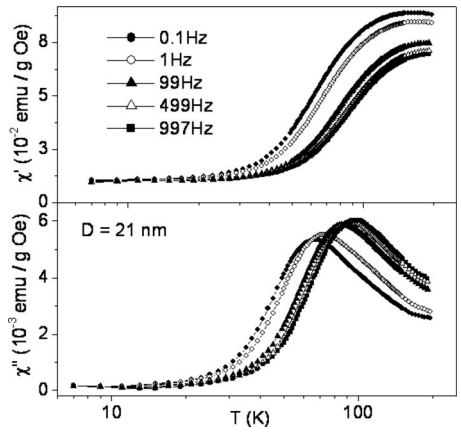

FIG. 2. Experimental χ' and χ'' vs T for $D=21$ nm at five frequencies shown.

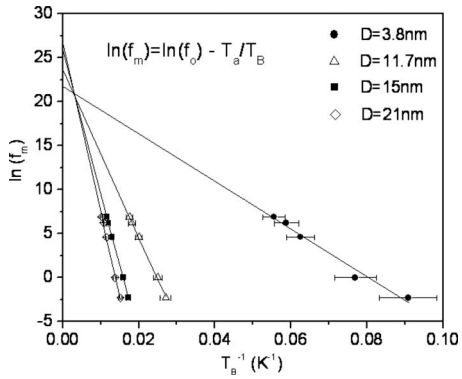

FIG. 3. Plots of $\ln f_m$ against T_B^{-1} to determine f_o and T_a from the equation $f_m=f_o \exp(-T_a/T_B)$. The solid lines are least-squares fits to the data.

for the $D=3.8$ nm sample and $f_o=1.82(^{+0.94}_{-0.62})\times 10^{10}$ Hz, $f_o=1.72(^{+0.25}_{-0.23})\times 10^{11}$ Hz, and $f_o=3.96(^{+4.62}_{-2.13})\times 10^{11}$ Hz for the $D=11.7$ nm, $D=15$ nm, and $D=21$ nm samples, respectively. For the two larger particles, the magnitude of f_o is higher by an order of magnitude. Since the presence of IPI often leads to increased magnitudes of f_o (Ref. 11) when data are fit to Eq. (6), we next evaluated the parameter $\Phi = \Delta T_B/[T_B \Delta \log_{10} f_m]$, which represents fractional change in T_B per decade change in f_m.[12] Experiments have shown that Φ is very small (0.005–0.05) for spin glasses and $\Phi \geq 0.13$ for isolated noninteracting NPs.[12] For intermediate values of Φ ($0.05<\Phi<0.13$), IPI is present with its effect decreasing with increase in Φ. Determining ΔT_B for maximum and minimum f_m in our experiments, $\Phi=0.16$, 0.13, 0.12, and 0.12 are found respectively for the $D=3.8$, 11.7, 15, and 21 nm samples. These magnitudes of Φ suggest the presence of a weak IPI in the larger $D=15$ nm and $D=21$ nm particles (possibly due to larger moment per particle) and absence of IPI in the two smaller particles. Thus it is very likely that the larger magnitudes of f_o in the two larger NPs is due to the presence of IPI as the magnitudes of $T_o>0$ determined below also suggest. Taking into consideration the relatively large uncertainty in f_o for the smallest $D=3.8$ nm NPs, we have chosen $f_o=1.82\times 10^{10}$ Hz for the $D=11.7$ nm NPs as the likely magnitude for f_o for this system. Using this magnitude of f_o, the data are plotted as T_B against $1/\ell n(f_o/f_m)$ in Fig. 4 to check the validity of Eq. (7). The least-squares fits are then used to determine T_o and T_a. It is evident that T_o is

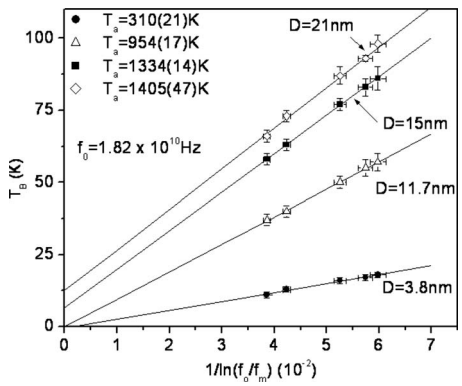

FIG. 4. Plots of T_B vs $1/\ln(f_o/f_m)$ following Eq. (7) for the f_o value noted on the figure. The lines through the points are least-squares fits with magnitudes of T_a shown.

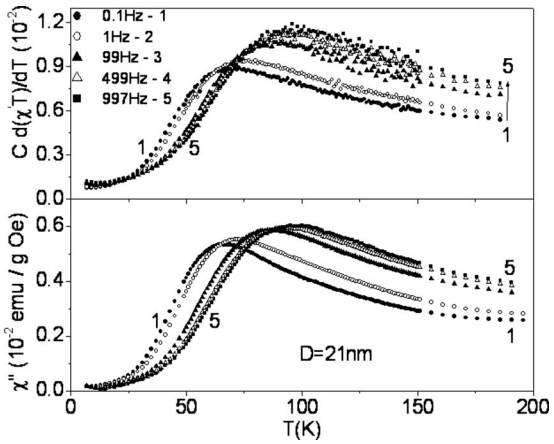

FIG. 5. Plots of experimental χ'' vs T and computed $C\partial(\chi' T)/\partial T$ of Eq. (7) using the data of the $D=21$ nm sample.

zero within experimental uncertainties for the two smaller NPs and $T_o=6.6(0.7)$ K and 12.5(2.5) K, respectively, for the $D=15$ nm and $D=21$ nm samples. Also T_a representing the energy barrier increases with increase in the size D of the NPs (see Fig. 4). In an earlier publication, we reported $f_o=2.6\times10^9$ Hz for the $D=3.8$ nm sample using an eye-ball fit of the data[7] similar to the value of $f_o=1.8\times10^9$ Hz reported by Goya *et al.*[13] in a 5% Ni/SiO_2 sample. This value is consistent with $f_o=1.82\times10^{10}$ Hz used here since for $f_o=2.8\left(^{+11.6}_{-2.2}\right)\times10^9$ Hz determined above using least-squares fitting has large enough uncertainty to accommodate $f_o=1.82\times10^{10}$ Hz. The important result of this analysis is that using a size independent f_o, the presence of measurable IPI is evident in the two larger sizes and T_a increases with increase in the size of D of the NPs as qualitatively expected. Later we show that the magnitude of $f_o=1.8\times10^{10}$ Hz determined above is consistent with calculations also using a theoretical expression.

Next, the magnitudes of $T_a=K_aV/k$ are used to determine K_a representing the energy barrier assuming spherical NPs. For the cubic anisotropy of Ni, $K_a=K_1/12$, where K_1 is the first-order anisotropy constant with $K_1=|7.5|\times10^5$ ergs/cm^3 for bulk Ni.[14] The computed values of $|K_1|$ (in units of 10^5 ergs/cm^3) are 178.7, 18.8, 12.5, and 4.8 for the $D=3.8$, 11.7, 15, and 21 nm samples, respectively. The observed increase in K_1 with decreasing D has been reported and discussed in other systems also, the source being increasing surface anisotropy with decreasing D.[3–6] For the largest $D=21$ nm sample, the magnitude of K_1 is close to the value for bulk Ni.

To test the validity of the correlation between χ'' and $C\partial(\chi' T)/\partial T$ predicted by Eq. (8), the plots of the experimental χ'' and computed $C\partial(\chi' T)/\partial T$ versus T are shown in Fig. 5 using the χ' versus T data for our representative sample with $D=21$ nm. All primary features of experimental χ'' such as the frequency and T dependence, are also evident in the plots of $C\partial(\chi' T)/\partial T$, except that the peak magnitudes are off by a factor of about 2. This discrepancy is likely related to the approximations made in deriving the magnitude of C in Eq. (8).[2] Comparison of χ'' and computed $C\partial(\chi' T)/\partial T$ for the other three samples yielded similar results. It may be relevant to note that in bulk antiferromagnets near the Néel temperature, $\partial(\chi' T)/\partial T$ is proportional to the specific heat.[15]

Next we calculate the theoretically expected magnitude of the attempt frequency f_o. Based on the earlier work by Brown,[16] a simplified expression for f_o in zero field given by Aharoni[17] for the case of $T_a \gg T$, reduces to the following for the case of Ni:

$$f_o=[T_a/\pi T]^{1/2}\gamma_o K_1/6M_s. \tag{9}$$

Here γ_o is the gyromagnetic ratio and M_s is the saturation magnetization. For Ni with $g=2.2$, $\gamma_o=2\pi g\mu_B/h=1.935\times10^7$. For T in Eq. (9), we use the average T_B measured at the frequencies f_m used in our experiments since f_o was determined at these temperatures and the condition $T_a \gg T$ is still valid using the T_a values noted in Fig. 4. We used the values of $M_s=245$, 216, 229, and 274 emu/cm^3 measured at 5 K for the $D=3.8$, 11.7, 15, and 21 nm samples, respectively. These magnitudes of M_s are only about 50% of the corresponding magnitude for bulk Ni, likely due to disorder of spins on the surface of a NP. For the $D=3.8$ nm sample with $T_a=310$ K, Eq. (9) yields $f_o=6.0\times10^{11}$ Hz. Similar calculations for the other samples yield the following f_o values: 7.1×10^{10} Hz for 11.7 nm, 4.2×10^{10} Hz for 15 nm, and 1.3×10^{10} Hz for 21 nm. Except for the smallest NPs, these calculated magnitudes of f_o using Eq. (9) compare quite favorably with $f_o=1.8\times10^{10}$ Hz derived from the analysis of the data.

In summary, the variations of the magnetic relaxation parameters T_B and T_a with size of Ni NPs dispersed in silica matrix are shown to follow the predictions of Eqs. (1)–(8) with a size independent f_o and the presence of a weak IPI in the larger NPs. The order of magnitude of the calculated f_o is in agreement with the measured f_o.

The research at West Virginia University was supported in part by U.S. Department of Energy (Contract No. DE-FC-26-05NT42456).

[1] L. Néel, Ann. Geophys. **5**, 99 (1949).
[2] L. Lundgren, P. Svedlindh, and O. Beckman, J. Magn. Magn. Mater. **25**, 33 (1981).
[3] F. Bødker, S. Morup, and S. Linderoth, Phys. Rev. Lett. **72**, 282 (1994).
[4] K. Gilmore, Y. U. Idzerda, M. T. Klem, M. Allen, T. Douglas and M. Young, J. Appl. Phys. **97**, 10B301 (2005).
[5] R. Yanes, O. C. Fesenko, H. Kachkachi, D. A. Garanin, R. Evans, and R. W. Chantrell, Phys. Rev. B **76**, 064416 (2007).
[6] H. Shim, P. Dutta, M. S. Seehra, and J. Bonevich, Solid State Commun. **145**, 192 (2008).
[7] V. Singh, M. S. Seehra and J. Bonevich, J. Appl. Phys. **103**, 07D524 (2008).
[8] J.-O. Andersson, C. Djurberg, T. Jonsson, P. Svedlindh, and P. Nordblad, Phys. Rev. B **56**, 13983 (1997).
[9] S. Shtrikman and E. P. Wohlfarth, Phys. Lett. **85A**, 467 (1981).
[10] J. L. Tholence, Solid State Commun. **88**, 917 (1993).
[11] H. Shim, A. Mannivannan, M. S. Seehra, K. M. Reddy and A. Punnoose, J. Appl. Phys. **99**, 08Q503 (2006) and references therein.
[12] J. L. Dormann, L. Bessais, and D. Fiorani, J. Phys. C **21**, 2015 (1988).
[13] G. F. Goya, F. C. Fonseca, R. F. Jardim, R. Muccillo, N. L. V. Carreno, E. Longo, and E. R. Leite, J. Appl. Phys. **93**, 6531 (2003).
[14] J. I. Gittleman, B. Abeles, and S. Bozowski, Phys. Rev. B **9**, 3891 (1974).
[15] E. E. Bragg and M. S. Seehra, Phys. Rev. B **7**, 4197 (1973); M. E. Fisher, Philos. Mag. **7**, 1731 (1962).
[16] W. F. Brown, Jr., J. Appl. Phys. **34**, 1319 (1963).
[17] A. Aharoni, Phys. Rev. B **7**, 1103 (1973).